Electronic Communication Mediated by a $Pt^{I}-Pt^{I}$ σ-Bond

John H. K. Yip,*,† Jianguo Wu,† Kwok-Yin Wong,*,‡ Kam Piu Ho,‡ Christine So-Ngan Pun,‡ and Jagadese J. Vittal†

Department of Chemistry, The National University of Singapore, 10 Kent Ridge Crescent, 119260 Singapore, and Department of Applied Biology and Chemical Technology, Hong Kong Polytechnic University, Hunghom, Kowloon, Hong Kong SAR, People's Republic of China

Received July 1, 2002

A binuclear complex $[Pt_2(dppm)_2(C{\equiv}CFc)_2]$ (**1**) (dppm = bis(diphenylphosphino)methane, Fc = $C_5H_5Fe^{II}C_5H_4$, ferrocenyl) containing two redox-active ferrocenylacetylides linked by a $Pt^{I}-Pt^{I}$ σ-bond is designed to probe electronic communication through a C≡C−Pt−Pt−C≡C linkage. The X-ray crystal structure of the complex shows a Pt−Pt bond distance of 2.7023(2) Å and a Fe−Fe separation of 14.474(2) Å. The cyclic voltammogram (CV) of **1** displays two quasi-reversible one-electron Fc oxidations ($\Delta E_p \approx 70$ mV at 20 mV s^{-1}, $i_{pc}/i_{pa} \approx 1$) separated by 267 ± 10 mV, and accordingly the equilibrium constant for the comproportionation $\mathbf{1}^{2+} + \mathbf{1} \leftrightarrow 2\ \mathbf{1}^{+}$ is estimated to be $(3.3 \pm 1.5) \times 10^4$. These suggest considerable electronic communication between the redox centers in the mixed-valence complex $\mathbf{1}^{+}$. The UV−vis−NIR absorption spectrum of **1** shows an intervalence-charge-transfer band at 11 300 ± 50 cm^{-1} ($\epsilon_{max} = 610 \pm 10\ M^{-1}\ cm^{-1}$), and the electronic coupling parameter H_{AB} is estimated to be 190 ± 20 cm^{-1}. Addition of d^{10} $Au^{I}Cl$ and $Au^{I}Br$ fragments to the Pt−Pt bond gives rise to two A-frame clusters $[Pt_2(\mu\text{-AuX})(dppm)_2(C{\equiv}CFc)_2]$ (X = Cl or Br), whose X-ray crystal structures are composed of isosceles triangles of Pt_2Au. In contrast to **1**, electronic communication through the Pt_2Au cluster is very weak, as the CVs of the compounds exhibit no splitting of Fc oxidations. Possible reasons for the shutdown of electronic communication are discussed.

Introduction

Mixed-valence complexes continue to command the attention of chemists.[1] While they were first treated as models for intramolecular electron transfer,[2] the compounds were recently regarded as prototypes for molecular switches[1a,3] and wires.[1e,4] Even in the early days of modern mixed-valence chemistry, the crucial role played by the bridge in mediating electron delocalization was fully recognized.[5] The question of how its geometry and electronic structure affect the ground state electronic communication between the metal centers has been addressed theoretically[6] and experimentally.[7] Recent attempts to understand how metal ions mediate charge delocalization led to syntheses of mixed-valence complexes that contain metal ions as part of their spacers.[8,9] Examples are *trans*-$[Pt^{II}(PPh_3)_2(C{\equiv}CFc)_2]$[8] (C≡CFc = ferrocenylacetylide, Fc = $C_5H_5Fe^{II}C_5H_4$) and *trans*-$[Ru^{II}(dppm)_2(C{\equiv}CFc)_2]$.[9a−c] Furthermore, metal[10] and main group[11] clusters were also incorporated into the linkers of mixed-valence complexes. Notably a

* To whom correspondence should be addressed. Fax: 65-67791691. E-mail: chmyiphk@nus.edu.sg.
† The National University of Singapore.
‡ Hong Kong Polytechnic University.

(1) For recent reviews, see: (a) Astruc, D. *Acc. Chem. Res.* **1997**, *30*, 383. (b) McCleverty, J. A.; Ward, M. D. *Acc. Chem. Res.* **1998**, *31*, 842. (c) Kaim, W.; Klein, A.; Glöckle, M. *Acc. Chem. Res.* **2000**, *33*, 755. (d) Barlow, S.; O'Hara, D. *Chem. Rev.* **1997**, *97*, 637. (e) Paul, F.; Lapinte, C. *Coord. Chem. Rev.* **1998**, *180*, 431. (f) Demadis, K. D.; Hartshorn, C. M.; Meyer, T. J. *Chem. Rev.* **2001**, *101*, 2655.

(2) (a) Meyer, T. J.; Taube, H. *In Comprehensive Coordination Chemistry*; Wilkinson, G., Guilard, R., Mclafferty, J. A., Eds.; Pergamon Press: Oxford, 1987; Vol. 1, Chapter 7.2, p 331. (b) Gordon, B. N.; Williams, L. L.; Sutin, N. *J. Am. Chem. Soc.* **1961**, *83*, 2061.

(3) (a) Steenwinkel, P.; Grove, D. M.; Veldman, N.; Spek, A. L.; van Koten, G. *Organometallics*, **1998**, *17*, 5647. (b) Ward, M. D. *Chem. Soc. Rev.* **1995**, 121. (c) Laine, P.; Marvaud, V.; Gourdon, A.; Launay, J.-P.; Argazzi, R.; Bignozzi, C.-A. *Inorg. Chem.* **1996**, *35*, 711.

(4) (a) Paul, F.; Meyer, W. E.; Toupet, L.; Jiao, H. J.; Gladysz, J. A.; Lapinte, C. *J. Am. Chem. Soc.* **2000**, *122*, 9405. (b) Rigaut, S.; Le Pichon, L.; Daran, J. C.; Touchard, D.; Dixneuf, P. H. *J. Chem. Soc., Chem. Commun.* **2001**, 1206. (c) Long, N. J.; Martin, A. J.; Vilar, R.; White, A. J. P.; Williams, D. J.; Younus, M. *Organometallics* **1999**, *18*, 4261. (d) Zhu, Y. B.; Wolf, M. O. *J. Am. Chem. Soc.* **2000**, *122*, 10121. (e) Hradsky, A.; Bildstein, B.; Schuler, N.; Schottenberger, H.; Jaitner, P.; Ongania, K.-H.; Wurst, K.; Launay, J.-P. *Organometallics* **1997**, *16*, 392. (f) Le Stang, S.; Paul, F.; Lapinte, C. *Organometallics* **2000**, *19*, 1035.

(5) (a) Creutz, C.; Taube, H. *J. Am. Chem. Soc.* **1973**, *95*, 1086. (b) Richardson, D. E.; Taube, H. *Coord. Chem. Rev.* **1984**, *60*, 107. (c) Creutz, C. In *Progress in Inorganic Chemistry*; Lippard, S. J., Ed.; Wiley: New York 1983; Vol. 30, p 1.

(6) (a) Hush, N. S. *Prog. Inorg. Chem.* **1967**, *8*, 391. (b) Hush, N. S. *Coord. Chem. Rev.* **1985**, *64*, 135. (c) Wong, K. Y.; Schatz, P. N. *Prog. Inorg. Chem.* **1967**, *8*, 391. (d) Crutchley, R. J. *Adv. Inorg. Chem.* **1994**, *41*, 273. (e) Evans, C. E. B.; Naklicki, M. L.; Rezvani, A. R.; White, C. A.; Kondratiev, V. V.; Crutchley, R. J. *J. Am. Chem. Soc.* **1998**, *120*, 13096. (f) Patoux, C.; Coudret, C.; Launay, J.-P.; Joachim, C.; Gourdon, A. *Inorg. Chem.* **1997**, *36*, 5037.

(7) (a) Atwood, C. P.; Geiger, W. E. *J. Am. Chem. Soc.* **2000**, *122*, 5477. (b) Cargill Thompson, A. M. W.; Gatteschi, D.; McCleverty, J. A.; Navas, J. A.; Rentschler, E.; Ward, M. D. *Inorg. Chem.* **1996**, *35*, 2701. (c) Rittinger, S.; Buchholz, D.; Delville-Desbois, M. H.; Linares, J.; Varret, F.; Boese, R.; Zsolnai, L.; Huttner, G.; Astruc, D. *Organometallics* **1992**, *11*, 1454. (d) Dong, T. Y.; Chang, C. K.; Lee, S. H.; Lai, L. L.; Chiang, M. Y. N.; Lin, K. J. *Organometallics* **1997**, *16*, 5816. (e) Ribou, A. C.; Launay, J.-P.; Sachtleben, M. L.; Li, H.; Spangler, C. W. *Inorg. Chem.* **1996**, *35*, 3735. (f) Barlow, S.; Murphy, V. J.; Evan, J. S. O.; O'Hara, D. *Organometallics* **1995**, *14*, 3461. (g) Levanda, C.; Bechgaard, K.; Cowan, D. O. *J. Org. Chem.* **1976**, *41*, 2700.

(8) (a) Osella, D.; Gambino, O.; Nervi, C.; Ravera, M.; Russo, M. V.; Infante, G. *Inorg. Chim. Acta* **1994**, *225*, 35. (b) Osella, D.; Gobetto, R.; Nervi, C.; Ravera, M.; D'Amato, R.; Russo, M. V. *Inorg. Chem. Commun.* **1998**, *1*, 239.

10.1021/om020513+ CCC: $22.00
Publication on Web 10/25/2002

Scheme 1

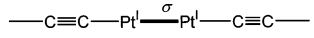

hexanuclear rhodium cluster was shown to enhance electronic communication between two C_{60} molecules in a recent study.[10d] On the other hand, our study on $[Cu_3(dppm)_3(C{\equiv}CFc)_2]^+$, a trinuclear cuprous cluster capped by two FcC≡C groups, showed that the Cu^I_3 cluster does not facilitate charge delocalization, and stability of the mixed-valence complex $[Cu_3(dppm)_3(C{\equiv}CFc)_2]^{2+}$ is mostly due to reduction of electrostatic repulsion and statistical distribution.[10e] Related work includes investigations on charge delocalization in Fc-C≡C−C≡C−Fc, whose backbone is modified with Os_3CO_9 clusters.[12]

Whereas the studies of the charge delocalization over metal clusters have been initiated, the related question of how a *single* metal−metal bond mediates electronic communication has not been fully addressed. It is pertinent because single[13] and tandem metal−metal bonds[14] have been suggested to be potential molecular wires. In view of this, we embarked on a study of electronic communication mediated by a metal−metal bond. While the order of metal−metal bonds varies from one to four,[15] we focused on the supposedly simplest one, namely, the single σ-bond. A metal−metal σ-bond is found in binuclear complexes with a ground state electronic configuration of d^7-d^7 (e.g., $Pt^{III}-Pt^{III}$, $Rh^{II}-Rh^{II}$) and d^9-d^9 (e.g., Pd^I-Pd^I, Pt^I-Pt^I, $Au^{II}-Au^{II}$).[15] In this study, the Pt^I-Pt^I σ-bond[16] was chosen first because polymers composed of C≡C−Pt−Pt−C≡C linkages (Scheme 1) were suggested to be prototypes for conducting materials.[17] Second, Pt^I-Pt^I complexes are known to react with d^{10} metals such as Au^II[18] and $Hg^{II}Cl_2$[19] to form trinuclear Pt_2Au and Pt_2Hg clusters. This unique reactivity of the Pt^I-Pt^I bond allows the electronic structure of the bond and its ability to conduct electronic communication to be perturbed. With all these in mind, we synthesized the complex $[Pt^I_2(dppm)_2(C{\equiv}CFc)_2]$ (dppm = bis(diphenylphosphino)methane, Fc = ferrocenyl) (**1**), which consists of a linear array of two ferrocenylacetylides and a Pt−Pt bond. In addition, two gold(I) adducts of **1**, $[Pt^I_2(\mu\text{-AuX})(dppm)_2(C{\equiv}CFc)_2]$ [X = Cl (**2**) and Br (**3**)], were prepared. Electrochemical and spectroscopic studies of the complexes revealed intriguing differences between the Pt_2Au cluster and Pt^I-Pt^I in transmitting electronic interactions.

Experimental Section

General Methods. All reactions were carried out in a N_2 atmosphere unless otherwise noted. Solvents used in spectroscopic and electrochemical measurements were purified according to the literature methods. $[Pt_2(dppm)_2Cl_2]$,[20] ethylnylferrocene[21] and ferrocenium hexafluorophosphate[22] were prepared following the reported methods. Me_2SAuCl and Me_2SAuBr were synthesized from the reactions of Me_2S (2 molar equiv) and $KAuCl_4$ and $AuBr_3$ in ethanol, respectively.

Physical Measurements. ^1H and ^{31}P NMR spectra were recorded at 25 °C on a Bruker ACF 300 spectrometer. UV−vis and near-infrared absorption spectra were recorded on a Perkin-Elmer Lambda 900 UV/vis/NIR spectrometer. Elemental analyses were carried out in the microanalysis laboratory in the Department of Chemistry, the National University of Singapore. IR spectra (KBr) were recorded using a Bio-Rad Win-IR spectrophotometer. A Bioanalytical Systems (BAS) model 100W electrochemical analyzer was used in all electrochemical measurements. n-Bu_4NPF_6 (0.1 M) was used as the supporting electrolyte unless otherwise stated. Cyclic voltammetry and differential pulse voltammetry were performed in a conventional two-compartment electrochemical cell. The glassy carbon disk working electrode (area 0.07 cm^2) was treated by polishing with 0.05 μm alumina on a microcloth and then sonicated for 5 min in deionized water followed by rinsing with the solvent used in the electrochemical studies. An $Ag/AgNO_3$ (0.1 M in CH_3CN) electrode was used as reference electrode. The half-wave potential ($E_{1/2}$) values are the average of the cathodic and anodic peak potentials for the oxidative and reductive waves of reversible couples.[23a] The potential of the Pt complexes was always referenced to the half-wave potential of the ferrocenium/ferrocene (FcH^+/FcH) couple as the internal reference.[23b]

Synthesis of $[Pt_2(dppm)_2(C{\equiv}CFc)_2]$ (1). To a methanol solution (250 mL) of ethynylferrocene (0.40 g, 1.9 mmol) and sodium (0.044 g, 1.9 mmol) was added $[Pt_2(dppm)_2Cl_2]$ (1.0 g, 0.818 mmol), and the mixture was stirred at room temperature for 12 h and then filtered. The filtrate was concentrated before addition of excess diethyl ether to precipitate the product as an orange solid. Pure product was obtained by diffusing diethyl ether into a dichloromethane solution of the solid. Yield: 43%. Anal. Calcd (%) for $C_{74}H_{63}Cl_2FeP_4Pt_2$: C, 56.3; H, 3.9. Found (%): C, 55.7; H, 4.1. ^1H NMR (300 MHz, $CDCl_3$, δ/ppm): 3.31−3.86 (m, 18H, Cp); 4.95 (m, 4H, PCH_2P); 7.15−7.58 (m, 40H,

(9) (a) Colbert, M. C. B.; Lewis, J.; Long, N. J.; Raithby, P. R.; White, A. J. P.; Williams, D. J. *J. Chem. Soc., Dalton Trans.* **1997**, 99. (b) Zhu, Y.; Clot, O.; Wolf, M. O.; Yap, G. P. A. *J. Am. Chem. Soc.* **1998**, *120*, 1812. (c) Jones, N. D.; Wolf, M. O.; Giaquinta, D. M. *Organometallics* **1997**, *16*, 1352. (d) Glaser, T.; Beissel, T.; Bill, E.; Weyhermüller, T.; Schünemann, V.; Meyer-Klaucke, W.; Trautwein, A. X.; Wieghardt, K. *J. Am. Chem. Soc.* **1999**, *121*, 2193. (e) Back, S.; Rheinwald, G.; Lang, H. *Organometallics* **1999**, *18*, 4119.

(10) (a) Zhu, N.; Pebler, J.; Vahrenkamp, H. *Angew. Chem., Int. Ed. Engl.* **1996**, *35*, 894. (b) McAdam, C. J.; Duffy, N. W.; Robinson, B. H.; Simpson, J. *Organometallics* **1996**, *15*, 3935. (c) Osella, D.; Nervi, C.; Ravera, M.; Duffy, N. W.; McAdam, C. J.; Robinson, B. H.; Simpson, J. *Inorg. Chim. Acta* **1996**, *247*, 99. (d) Lee, K.; Song, H.; Kim, B.; Park, J. T.; Park, S.; Choi, M.-G. *J. Am. Chem. Soc.* **2002**, *124*, 2872. (e) Yip, J. H. K.; Wu, J.; Wong, K.-Y.; Yeung, K.-W.; Vittal. J. J. *Organometallics* **2002**, *21*, 1612.

(11) Fox, M. A.; Paterson, M. A. J.; Nervi, C.; Galeotti, F.; Puschmann, H.; Howard, J. A. K.; Low, P. J. *J. Chem. Soc., Chem. Commun.* **2001**, 1610.

(12) (a) Adams, R. D.; Qu, B. *Organometallics* **2000**, *19*, 2411. (b) Adams, R. D.; Qu, B. *Organometallics*, **2000**, *19*, 4090. (c) Adams, R. D.; Kwon, O.-S.; Qu, B.; Smith, M. D. *Organometallics* **2001**, *20*, 5225.

(13) Berry, J. F.; Cotton, F. A.; Daniels, L. M.; Murillo, C. A. *J. Am. Chem. Soc.* **2002**, *124*, 3212.

(14) (a) Yang, M. H.; Lin, T. W.; Chou, C. C.; Lee, H. C.; Chang, H. C.; Lee, G. H.; Leung, M. K.; Peng, S. M. *Chem. Commun.* **1997**, 2279. (b) Cotton, F. A.; Daniels, L. M.; Murillo, C. A.; Pascual, I. *J. Am. Chem. Soc.* **1997**, *119*, 10223 (c) Shieh, S. J.; Chou, C. C.; Lee, G. H.; Wang, C. C.; Peng, S. M. *Angew. Chem., Int. Ed. Engl.* **1997**, *36*, 56. (d) Lai, S.-Y.; Lin, T.-W.; Chen, Y.-H.; Wang, C.-C.; Lee, G.-H.; Yang, M.-H.; Leung, M.-k.; Peng, S.-M.; *J. Am. Chem. Soc.* **1999**, *121*, 250.

(15) Cotton, F. A.; Walton, R. A. *Multiple Bonds Between Atoms*, 2nd ed.; Clarendon Press: Oxford, 1993.

(16) (a) Fisher, J. R.; Mills, A. J.; Sumner, S.; Brown, M. P.; Puddephatt, R. J.; Frew, A. A.; Manojloviæ-Muir, L.; Muir, K. W. *Organometallics* **1982**, *1*, 1421. (b) Khan, M. N. I.; King, C.; Wang, J.-C.; Wang, S.; Fackler, J. P., Jr. *Inorg. Chem.* **1989**, *28*, 4656. (c) Yip, H. K.; Che, C. M.; Peng, S. M. *J. Chem. Soc., Dalton Trans.* **1993**, 179.

(17) Irwin, M. J.; Jia, G.; Vittal, J. J.; Puddephatt, R. J. *Organometallics* **1996**, *15*, 5321.

(18) (a) Manojloviæ-Muir, L.; Muir, K. W.; Treurnicht, I.; Puddephatt, R. J. *Inorg. Chem.* **1987**, *26*, 2418. (b) Arsenault, G. J.; Manojloviæ-Muir, L.; Muir, K. W.; Treurnicht, I.; Puddephatt, R. J. *Angew Chem., Int. Ed. Engl.* **1987**, *26*, 86.

(19) Sharp, P. R. *Inorg. Chem.* **1986**, *25*, 4185.

(20) Brown, M. P.; Puddephatt, R. J.; Rashidi, M. *J. Chem. Soc., Dalton Trans.* **1977**, 951.

(21) Rodriquez, J.-G.; Oñate, A.; Martin-Villami, R. M.; Fonseca, I. *J. Organomet. Chem.* **1996**, *513*, 71.

(22) Connelly, N. G.; Geiger, W. E. *Chem. Rev.* **1996**, *96*, 877.

(23) (a) Gagné, R. R.; Koval, C. A.; Lisensky, G. C. *Inorg. Chem.* **1980**, *19*, 2855. (b) Gritzner, G.; Kùta, J. *Pure Appl. Chem.* **1982**, *54*.

Table 1. Crystal Data and Structure Refinements for 1·Et_2O, 2, and 3

	1·Et_2O	2	3
formula	$C_{78}H_{72}Fe_2OP_4Pt_2$	$C_{74}H_{62}AuFe_2ClP_4Pt_2$	$C_{74}H_{62}AuFe_2BrP_4Pt_2$
fw	1651.12	1809.41	1853.87
cryst syst	triclinic	triclinic	triclinic
space group	$P\bar{1}$	$P\bar{1}$	$P\bar{1}$
Z	2	2	2
cryst size (mm^3)	0.2 × 0.14 × 0.12	0.36 × 0.24 × 0.14	0.34 × 0.20 × 0.20
lattice params (Å)	a =11.7327(6),	a = 13.1768(8),	a = 13.2436(9),
	b = 16.1222(8),	b = 14.1641(9),	b = 14.1793(9),
	c = 17.7260(9)	c = 17.7187(1)	c = 17.8231(1)
	α = 89.990(1)°,	α = 89.858(1)°,	α = 89.494(1)°,
	β = 82.575(1)°,	β = 76.884(1)°,	β = 77.104(1)°,
	γ = 88.062(1)°	γ = 76.524(1)°	γ = 76.508(1)°
V ($Å^3$)	3322.9(3)	3127.6(3)	3169.2(4)
density(calc) (g cm^{-3})	1.650	1.921	1.943
abs coeff (mm^{-1})	4.767	7.436	7.927
F(000)	1632	1740	1776
no. of params varied	761	757	757
final R indices[a]	R1 = 0.0362	R1 = 0.0443	R1 = 0.0454
	wR2 = 0.0679	wR2 = 0.0842	wR2 = 0.0714
goodness of fit[b]	1.012	1.048	1.047

[a] $R1 = (||F_o| - |F_c||)/(|F_o|)$; $wR2 = [w(F_o^2 - F_c^2)/w(F_o^4)]^{1/2}$. [b] $GOF = [(w(F_o^2 - F_c^2)^2/(n - p)]^{1/2}$.

Ph). ^{31}P NMR (121.50 MHz, $CDCl_3$, δ/ppm): 0.81, $^1J(PtP)$ = 2945 Hz, $^3J(PtP)$ = −84 Hz, $^2J(P^AP^{A''})$ = 58 Hz, $^4J(P^AP^{A'''})$ = 24 Hz. IR (KBr): 2090 cm^{-1}, weak, ν(C≡C).

Synthesis of [Pt_2(μ-AuX)(dppm)$_2$(C≡CFc)$_2$] [X = Cl (2), Br (3)]. The same procedure was followed in the syntheses of **2** and **3**: To a 15 mL benzene solution of **1** (0.8 g, 0.5 mmol) was added 1 molar equiv of Me_2SAuCl (0.15 g) or Me_2SAuBr (0.17 g) dissolved in ∼8 mL of dicholoromethane, and the solution was stirred for 2 h at room temperature, during which its color changed to bright red. The solution was filtered, and addition of excess hexane to the filtrate precipitated the product as a red solid. Crystals of the compound was obtained by slow diffusion of diethyl ether into a dichloromethane solution of the complex. **2**: Yield: 55%. Anal. Calcd (%) for $C_{74}H_{62}AuClFe_2P_4Pt_2$: C, 49.1; H, 3.4. Found (%): C, 48.8; H, 3.7. ^1H NMR (300 MHz, $CDCl_3$, δ/ppm): 3.48−3.84 (m, 18H, Cp); 4.60 (m, 4H, PCH_2P); 7.22−7.95 (m, 40H, Ph). ^{31}P NMR (300 MHz, $CDCl_3$, δ/ppm): 11.39, $^1J(PtP)$ = 2483 Hz, $^3J(PtP)$ = −88 Hz, $^2J(P^AP^{A''})$ = 48 Hz, $^4J(P^AP^{A'''})$ = 10 Hz. IR (KBr): 2013 cm^{-1}, weak, ν(C≡C). **3**: Yield: 48%. Anal. Calcd (%) for $C_{74}H_{62}AuBrFe_2P_4Pt_2$: C, 47.9; H, 3.3. Found (%): C, 47.2; H, 3.3. ^1H NMR (300 MHz, $CDCl_3$, δ/ppm): 3.48−3.84 (m, 18H, Cp); 4.62 (m, 4H, PCH_2P); 7.17−7.93 (m, 40H, Ph). ^{31}P NMR (300 MHz, $CDCl_3$, δ/ppm): 11.23, $^1J(PtP)$ = 2483 Hz, $^3J(PtP)$ = −87 Hz, $^2J(P^AP^{A''})$ = 48 Hz, $^4J(P^AP^{A'''})$ = 10 Hz. IR (KBr): 2102 cm^{-1}, weak, ν(C≡C).

In Situ Preparation of 1^+. To a 3 mL dichloromethane solution of **1** was added excess ferrocenium hexafluorophate (1.6−3 molar equiv). The color of the solution changed from orange to deep brown, and it was stirred at room temperature for 0.5 h before being filtered into a quartz UV cell for spectroscopic measurements.

X-ray Crystallography. The diffraction experiments were carried out on a Bruker AXS SMART CCD three-circle diffractometer at T = 223 K, $2\theta-\omega$ scan with a sealed tube at 23 °C using graphite-monochromated Mo Kα radiation (λ = 0.71073 Å). The software used were SMART[24] for collecting frames of data, indexing reflection, and determination of lattice parameters; SAINT[24] for integration of intensity of reflections and scaling; SADABS[25] for empirical absorption correction; and SHELXTL[26] for space group determination, structure solution, and least-squares refinements on $|F|^2$. The crystals were mounted at the end of glass fibers and used for the diffraction experiments. Anisotropic thermal parameters were refined for the rest of the non-hydrogen atoms. The hydrogen atoms were placed in their ideal positions. A brief summary of crystal data and experimental details are given in Table 1. Crystallographic data 1·Et_2O: for the 51 762 reflections collected, 19 273 were independent (R_{int} = 0.0541). Index range: $-16 \le h \le 16$, $-22 \le k \le 22$, $-24 \le l \le 24$. Refinement of F^2 converged with R_1 = 0.0362 for $I > 2\sigma(I)$ and wR_2 = 0.0679. The residual electron density is 2.168 and −0.739 e $Å^{-3}$. **2**: $C_{74}H_{62}Fe_2AuClP_4Pt_2$, for the 46 642 reflections collected, 17 545 were independent (R_{int} = 0.0628). Index range: $-18 \le h \le 18$, $-19 \le k \le 19$, $-24 \le l \le 24$. Refinement of F^2 converged with R_1 = 0.0443 for $I > 2\sigma(I)$ and wR_2 = 0.0842. The residual electron density is 3.293 and −1.415 e $Å^{-3}$. **3**: $C_{74}H_{62}Fe_2AuBrP_4Pt_2$, for the 47 316 reflections collected, 17 757 were independent (R_{int} = 0.0648). Index range: $-18 \le h \le 18$, $-19 \le k \le 19$, $-24 \le l \le 25$. Refinement of F^2 converged with R_1 = 0.0454 for $I > 2\sigma(I)$ and wR_2 = 0.0714. The residual electron density is 2.960 and −1.328 e $Å^{-3}$.

Results

Structure of 1. The compound was synthesized from a substitution reaction between [Pt_2(dppm)$_2Cl_2$] and ethynylferrocene in the presence of sodium methoxide. Analogous to other dppm-bridged Pt^I_2 complexes,[16] the X-ray crystal structure of **1** shows a twisted $Pt_2(P-C-P)_2$ metallacycle (Figure 1 and Table 2a). The short Pt−Pt distance of 2.7023(2) Å signifies the presence of a single bond between the atoms (2.53−2.89 Å).[16] The metal−metal distance in Pt^I_2 complexes is known to be influenced by the ligands *trans* to the bond,[16c] and the same Pt−Pt distance exhibited by **1** and [Pt^I_2(dppm)$_2$(CN)$_2$] (2.704(1) Å)[16b] is in accord with the similar electronic properties of acetylide and cyanide. The Pt−C (2.055(4) and 2.021(4) Å) bond lengths compare favorably with other Pt-acetylides,[17] and the acetylene C−C distances (1.141(5) and 1.177(5) Å) are typical for a carbon−carbon triple bond. The Pt atoms and the two ferrocenylacetylide form a linear chain (C(21)−Pt(1)−Pt(2) = 178.46(1)°, C(23)−Pt(2)−Pt(1) = 179.61(1)°), and the two Fc groups are symmetric with respect to the Pt−Pt bond. The two iron atoms are widely separated by 14.474(2) Å. The solution $^{31}P\{^1H\}$ NMR spectrum of

(24) *SMART* & *SAINT* Software Reference Manuals, Version 4.0; Siemens Energy & Automation, Inc., Analytical Instrumentation: Madison, WI, 1996.

(25) Sheldrick, G. M. *SADABS*, a software for empirical absorption correction; University of Gottingen: Gottingen, Germany, 1996.

(26) *SHELXTL Reference Manual*, Version 5.03; Siemens Energy & Automation, Inc., Analytical Instrumentation: Madison, WI, 1996.

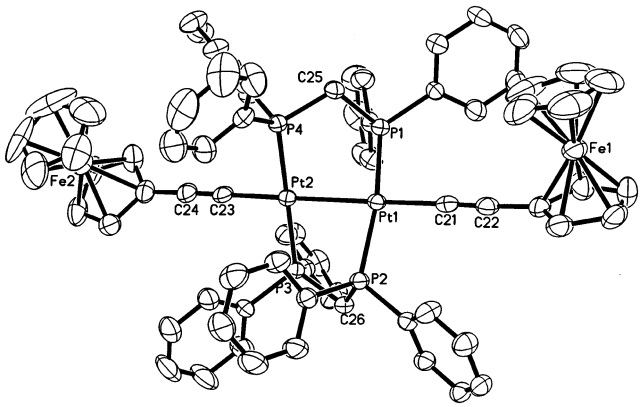

Figure 1. ORTEP drawing of **1**·Et_2O (H atoms and Et_2O are omitted for clarity, thermal ellipsoids are set at 50% probability level).

Table 2. Selected bond length (Å) and angles (deg) for 1·Et_2O, 2, and 3

a. **1**·Et_2O	
Pt(1)−Pt(2) 2.7023(2)	C(21)−Pt(1)−Pt(2) 178.46(1)
Pt(1)−C(21) 2.055(4)	C(23)−Pt(2)−Pt(1) 179.61(1)
Pt(2)−C(23) 2.021(4)	P(1)−Pt(1)−Pt(2) 83.27(3)
Pt(1)−P(1) 2.2510(9)	C(22)−C(21)−Pt(1) 178.6(4)
C(21)−C(22) 1.141(5)	C(24)−C(23)−Pt(2) 178.0(4)
C(23)−C(24) 1.177(5)	
b. **2**	
Pt(1)−Pt(2) 2.8077(3)	Pt(1)−Au(1)−Pt(2) 63.830(9)
Pt(1)−Au(1) 2.6395(3)	Au(1)−Pt(1)-Pt(2) 58.633(9)
Pt(2)−Au(1) 2.6712(3)	Au(1)−Pt(2)-Pt(1) 57.536(8)
Au(1)−Cl(1) 2.3151(9)	Cl(1)−Au(1)-Pt(1) 146.22(5)
Pt(1)−P(1) 2.2864(2)	C(1)−Pt(1)-Pt(2) 150.54(2)
Pt(1)−C(1) 1.988(6)	C(13)−Pt(2)-Pt(1) 149.66(2)
Pt(2)−C(13) 1.984(6)	C(1)−Pt(1)-Au(1) 150.42(2)
C(1)−C(2) 1.200(8)	C(14)−C(13)-Pt(2) 176.6(6)
	C(2)−C(1)-Pt(1) 172.4(5)
	P(2)−Pt(1)-P(1) 178.07(5)
c. **3**	
Pt(1)−Pt(2) 2.8019(4)	Pt(1)−Au(1)−Pt(2) 63.559(1)
Pt(1)−Au(1) 2.6786(4)	Au(1)−Pt(1)−Pt(2) 57.573(9)
Pt(2)−Au(1) 2.6413(4)	Au(1)−Pt(2)−Pt(1) 58.868(9)
Au(1)−Br(1) 2.4208(8)	Br(1)−Au(1)−Pt(1) 149.43(3)
Pt(1)−P(1) 2.2759(2)	C(1)−Pt(1)−Pt(2) 149.68(2)
Pt(1)−C(1) 2.077(7)	C(13)−Pt(2)−Pt(1) 149.44(2)
Pt(2)−C(13) 2.141(8)	C(1)−Pt(1)−Au(1) 152.72(2)
C(1)−C(2) 1.048(8)	C(14)−C(13)−Pt(2) 167.0(1)
	C(2)−C(1)−Pt(1) 176.3(7)
	P(2)−Pt(1)−P(1) 164.15(6)

1 shows signals arising from three isotopomers of the complex; the large negative ^3J(PtP) couple of −84 Hz is characteristics of Pt^I-Pt^I complexes.[16,20]

Electrochemistry of 1. The cyclic voltammogram (CV) of **1** measured in dichloromethane exhibits two quasi-reversible couples of similar size at half-wave potentials ($E_{1/2}$) of 8 ± 10 and 259 ± 10 mV in an anodic sweep ($\Delta E_p \approx 75$ and 64 mV for the two couples, respectively, at scan rate = 20 mV s^{-1}, $i_{pc}/i_{pa} \approx 1$ for scan rate 5−500 mV s^{-1}) (Figure 2a, all reduction potentials mentioned henceforth are referenced to the ferrocenium/ferrocene couple; i_{pc} and i_{pa} stand for cathodic and anodic peak currents, respectively). The couples are attributed to successive one-electron oxidations of the two ferrocenyl groups, as no counterpart was observed in the CV of $[Pt_2(dppm)_2Cl_2]$[16d] (Scheme 2).

The differences between cathodic and anodic potentials (ΔE_p) of the waves are close to the 60 mV expected for reversible one-electron oxidation[27] but increase as

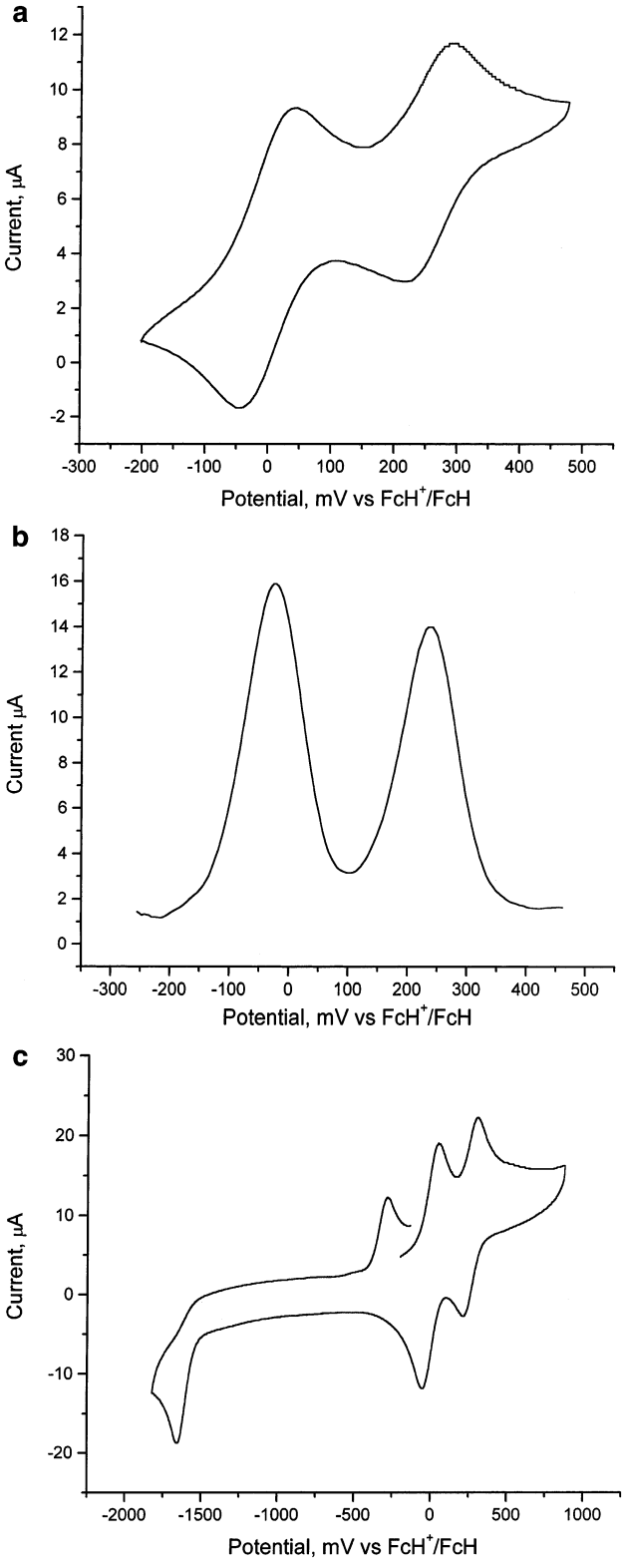

Figure 2. (a) Cyclic voltammogram of **1** (0.9 mM) in CH_2Cl_2 at a scan rate of 20 mV s^{-1}. Working electrode: glassy carbon (area = 0.07 cm^2), reference electrode: $Ag/AgNO_3$ (0.1M), supporting electrolyte: 0.1 M tetrabutylammonium hexafluorophosphate. The FcH^+/FcH couple is used as internal reference. All measurements were taken at room temperature (22 °C). (b) Differential pulse voltammogram of **1** (0.9 mM) in CH_2Cl_2; scan rate = 10 mV s^{-1}, sample width = 17 ms, pulse amplitude = 50 mV, pulse width = 50 ms, pulse period = 200 ms. (c) Extended cyclic voltammogram of **1** (0.9 mM) in CH_2Cl_2 showing cathodic scan. Conditions: same as those in part a.

Scheme 2

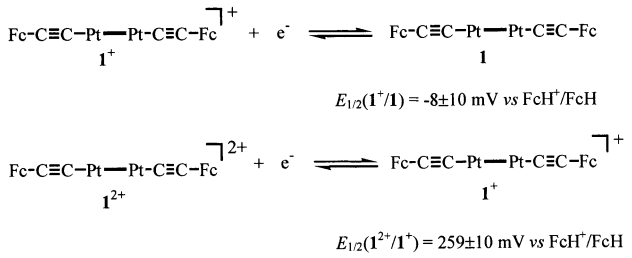

scan rate increases. A similar increase in ΔE_p with scan rate was observed for the FcH^+/FcH couple. The increase in ΔE_p with scan rate can be attributed to the relatively high resistance of the dichloromethane electrolyte used in CV measurements. The differential pulse voltammogram (DPV) of **1** exhibits two peaks of similar size with peak potential (E_p) at -27 ± 10 and 237 ± 10 mV, respectively (Figure 2b). Upon sweeping the potential in the cathodic direction, an irreversible reduction wave appears at -1.66 V; its anodic counterpart appears at -260 mV in the reverse scan (Figure 2c). The fact that the oxidation wave at -260 mV is due to a species generated in the -1.66 V reduction is evidenced by the observation that this oxidation wave does not appear if the scan is reversed at -1.0 V instead of -2.0 V. The irreversible processes do not affect the ferrocene oxidations.

The equilibrium constant K_c ($= [\mathbf{1}^+]^2/[\mathbf{1}][\mathbf{1}^{2+}]$) of the comproportionation between **1** and $\mathbf{1}^{2+}$ (reaction 1) is estimated to be $(3.3 \pm 1.5) \times 10^4$ using eq 1[5] ($\Delta E_{1/2} = E_{1/2}(\mathbf{1}^{2+}/\mathbf{1}^+) - E_{1/2}(\mathbf{1}^+/\mathbf{1}) = 267 \pm 14$ mV).

Reaction 1

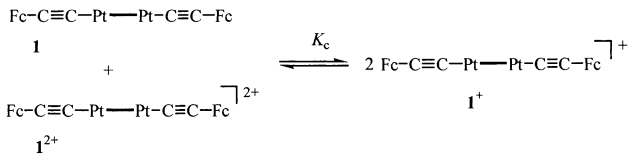

$$K_c = e^{(F/RT)\Delta E_{1/2}} \qquad (1)$$

Electronic Absorption Spectrum of $\mathbf{1}^+$. The extent of electron delocalization between the two Fc groups via the C≡C−Pt−Pt−C≡C linkage in $\mathbf{1}^+$ can be gauged by the electronic coupling parameter H_{AB}, obtainable for class II mixed-valence complexes from the intensity and bandwidth of their intervalence-charge-transfer (IVCT) transitions.[2a,5,6] Since attempts to isolate pure $\mathbf{1}^+$ were proved unsuccessful, the complex was generated in situ by reacting **1** with ferrocenium hexafluorophosphate ($FcH{\cdot}PF_6$), a mild and innocent oxidant,[22] which was chosen so as to avoid undesirable overoxidation to $\mathbf{1}^{2+}$ or decomposition. From the difference of the half-wave potentials of $\mathbf{1}^+/\mathbf{1}$ (-8 ± 10 mV vs FcH^+/FcH) and $FcH^{+}/FcH°$ couples, the equilibrium constant K_{ox} of reaction 2 is estimated to be 1.4 ± 0.5 ($K_{ox} = e^{(F/RT)\Delta E_{1/2}}$; $\Delta E_{1/2} = E_{1/2}(FcH^{+}/FcH°) - E_{1/2}(\mathbf{1}^+/\mathbf{1})$). The concentration of $\mathbf{1}^+$ can be calculated from eq 2.

(27) Bard, A. J.; Faulkner, L. R. *Electrochemical Methods*; John Wiley & Sons: New York, 1980; p 230.

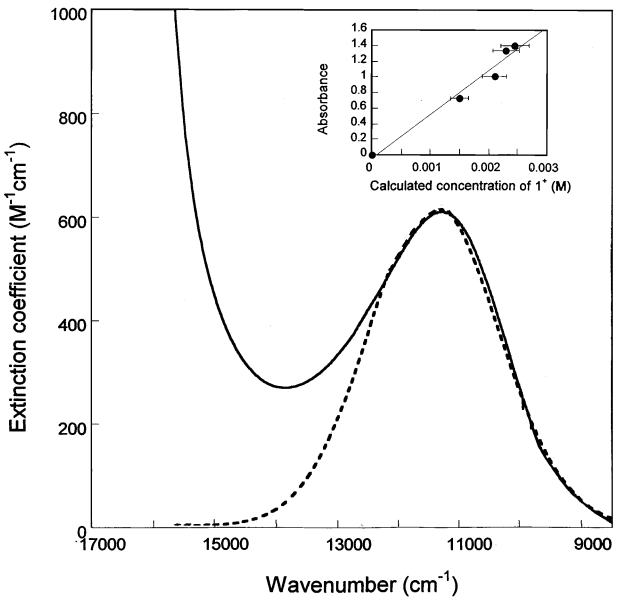

Figure 3. UV−vis−NIR absorption spectrum of $\mathbf{1}^+$ in CH_2Cl_2 at 297 K (inset: Beer plot of the absorbance of 11 300 cm^{-1} absorption vs the concentration of $\mathbf{1}^+$ as calculated from eq 2).

Reaction 2

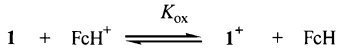

$$K_{ox} = 1.4 \pm 0.5 = \frac{[\mathbf{1}^+][FcH]}{[\mathbf{1}][FcH^+]} \qquad (2)$$

The small K_{ox} implies that $FcH{\cdot}PF_6$ cannot oxidize **1** to $\mathbf{1}^+$ stoichiometrically; hence excess $FcH{\cdot}PF_6$ is needed to generate sufficiently concentrated $\mathbf{1}^+$ solution for spectroscopic measurements. Virtually no $\mathbf{1}^{2+}$ would be produced even in the presence of a large excess of oxidant because the equilibrium constant of the second oxidation is exceedingly small ($= 4 \times 10^{-5}$). Similarly, disproportionation of $\mathbf{1}^+$ to **1** and $\mathbf{1}^{2+}$ is negligible, as the equilibrium constant for the reaction ($1/K_c$) is only $(3 \pm 1) \times 10^{-5}$.

Our study showed that adding excess $FcH{\cdot}PF_6$ (1.6−3 molar equiv) to a dichloromethane solution of **1** gives rise to a new absorption band maximized at 11 300 $\pm$ 50 cm^{-1} (ν_{max}). Gaussian fitting of the absorption band gives a half-height bandwidth $\Delta\nu_{1/2}$ of 2800 cm^{-1} (Figure 3). Since both ferrocenium and **1** show no absorption in the spectral region <16 000 cm^{-1}, the band is attributed to $\mathbf{1}^+$ produced in the oxidation. The absorbance of the band rises with increasing concentration of $FcH{\cdot}PF_6$. A straight line is obtained from a Beer plot of the absorbance against the equilibrium concentration of $\mathbf{1}^+$ as calculated from eq 2, confirming that the absorption arises from the mixed-valence complex (inset of Figure 3). From the gradient of the plot, the extinction coefficient ϵ_{max} of 610 $\pm$ 10 M^{-1} cm^{-1} is obtained. Poor solubility of **1** preludes the possibility of observing the absorption in solvents other than dichloromethane.

Structures of 2 and 3. Reacting **1** with one molar equiv of Me_2SAuX (X = Cl or Br) gave distorted A-frame complexes $[Pt_2(\mu\text{-}AuX)(dppm)_2(C{\equiv}CFc)_2]$ [X = Cl (**2**) Br (**3**)]. Single-crystal X-ray analysis revealed that **2** (Figure 4a) and **3** (Figure 4b) are basically isostructural,

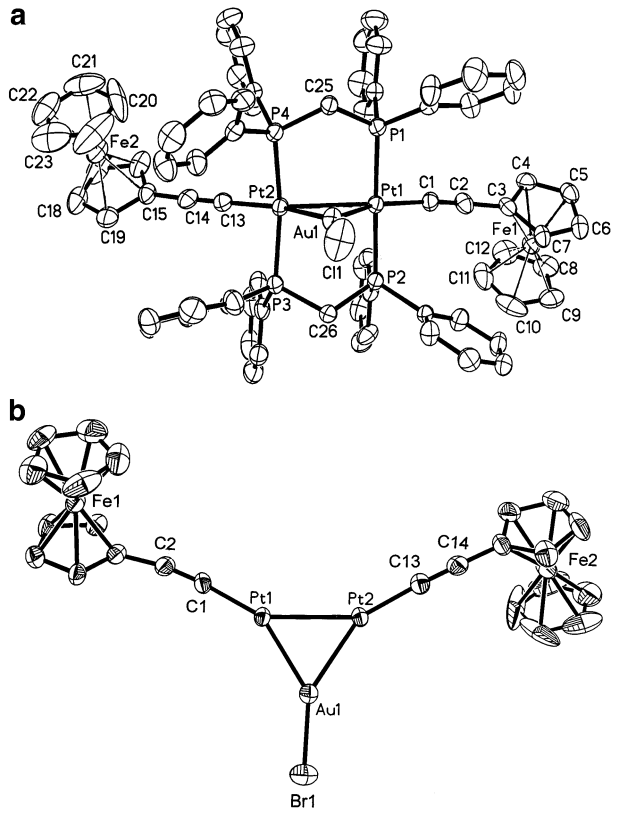

Figure 4. (a) ORTEP drawing of **2** (H atoms are omitted for clarity, thermal ellipsoids are set at 50% probability level). (b) Top view of complex **3** showing the Pt_2Au triangle (dppm are removed for clarity, thermal ellipsoids are set at 50% probability level).

showing very similar bond lengths and angles (for selected bond lengths and angles, see Table 2, b and c). Like the reported complex $[Pt_2(\mu\text{-AuI})(dppm)_2(C{\equiv}C\text{-}^tBu)_2]$,[18a] **2** and **3** are composed of Pt_2Au isosceles triangles in which the two Pt atoms are separated from the Au atom by ~2.65 Å. The Pt−Pt bonds are retained in **2** (2.8077(3) Å) and **3** (2.8019(4) Å) but slightly elongated, as seen in other Pt_2Au complexes. Unlike compound **1**, the two linearly coordinated ferrocenylacetylides (C(2)−C(1)−Pt(1) = 172.4(5)°) bend away from the Pt−Pt bond, showing C−Pt−Pt angles of 149.66(2)° and 150.54(2)° (**2**), respectively. The Pt−C and C≡C bond lengths of the complexes are close to those in **1**. The two Fc groups are symmetric with respect to the Pt_2Au cluster, showing an Fe−Fe distance of 13.958(3) Å. The ^{31}P NMR spectra of the complexes display signals from different isotopmers and large negative $^3J(PtP)$ coupling, which is typical for A-frame Pt_2Au and Pt_2Hg clusters.[18,19]

Electrochemistry of 2 and 3. In contrast to **1**, CVs of **2** ($E_{1/2}$ = −65 mV, ΔE_p = 100 mV at 20 mV s^{-1}, $i_{pc}/i_{pa} \approx 1$, Figure 5a) and **3** ($E_{1/2}$ = −74 mV, ΔE_p = 94 mV at 20 mV s^{-1}, $i_{pc}/i_{pa} \approx 1$, **SI**) show only one quasi-reversible wave, and their DPVs display only a single peak at −83 and −99 mV (Figures 5b and SI for **2** and **3**, respectively). No separation of waves is observed even at a slow scan rate of 5 mV s^{-1}. As there is no other quasi-reversible wave in the CVs and the reduction potentials of the waves are close to the Fc oxidations of **1**, the waves are assigned to the oxidations of the two Fc groups present in the complexes. In other words, the

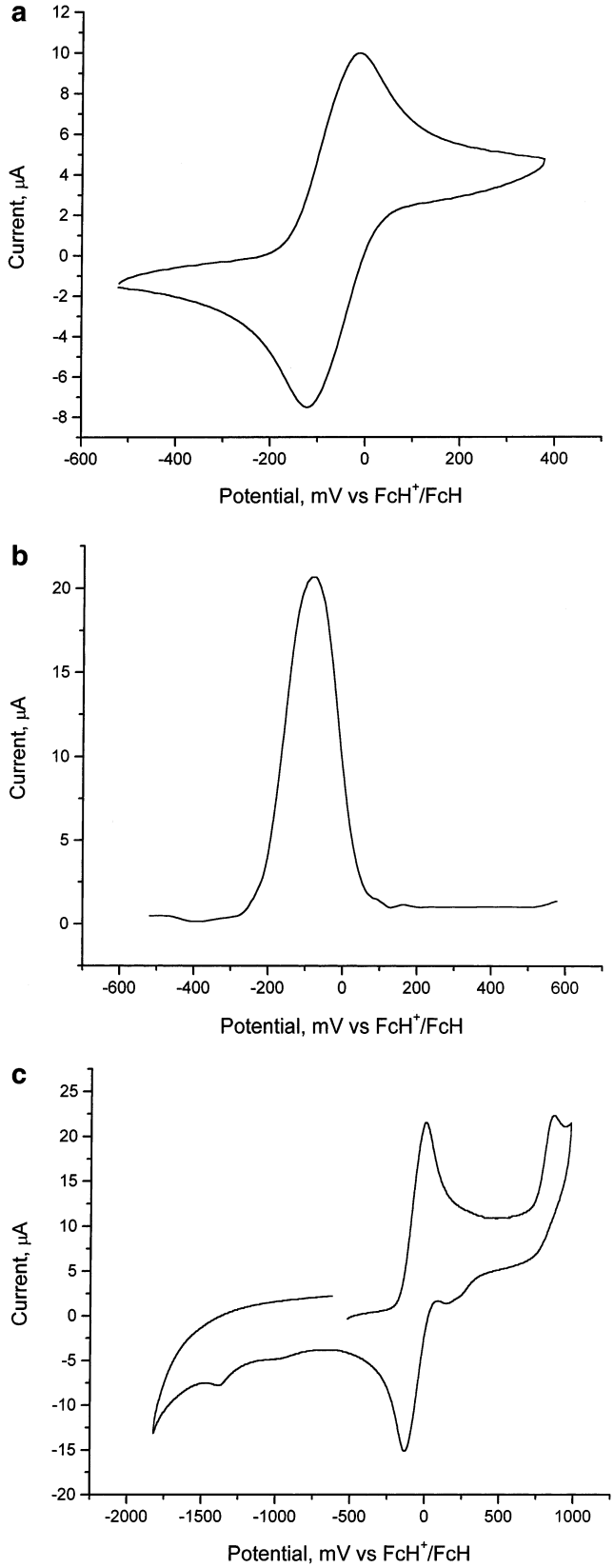

Figure 5. (a) Cyclic voltammogram of **2** (0.9 mM) in CH_2Cl_2 at a scan rate of 20 mV s^{-1}. Conditions: same as those in Figure 2a. (b) Differential pulse voltammogram of **2** (0.9 mM) in CH_2Cl_2; scan rate = 10 mV/s, sample width = 17 ms, pulse amplitude = 50 mV, pulse width = 50 ms, pulse period = 200 ms. (c) Cyclic voltammogram of **2** (0.9 mM) in CH_2Cl_2 showing extended anodic and cathodic scans, scan rate = 20 mV/s. Conditions: same as those in Figure 2a.

Table 3. Comproportionation Constants K_c of Bis(ferrocenylacetylide) Complexes

bis(ferrocenylacetylide)	$\Delta E_{1/2}$/mV	K_c	ref
$[Pt_2(dppm)_2(C{\equiv}CFc)_2]$ (**1**)	252	$(3.3\pm 1.5) \times 10^4$	this work
$[Pt_2(\mu\text{-AuX})(dppm)_2(C{\equiv}CFc)_2]$ (X = Cl, Br)	<70	<15	this work
trans-$\{[Pt[P(p\text{-tosyl})_3]_2(C{\equiv}CFc)_2]$	80	23	9a
trans,trans,trans-$[Ru(PBu_3)_2(CO)_2(C{\equiv}CFc)_2]$	90	35	9b
trans-$[Ru(dppm)_2(C{\equiv}CFc)_2]$	220	6100 ± 2500	9a,b,c
$[Cu_3(dppm)_3(C{\equiv}CFc)_2]$	110 ± 14	77 ± 30	10e
$FcC{\equiv}C{-}C{\equiv}C{-}Fc$	100	52	7g

two Fc oxidations ($\mathbf{2}^+/\mathbf{2}$ and $\mathbf{2}^{2+}/\mathbf{2}^+$ and $\mathbf{3}^+/\mathbf{3}$ and $\mathbf{3}^{2+}/\mathbf{3}^+$) in the complexes overlap and appear as a single wave. The fact that the couples resemble a single quasi-reversible one-electron oxidation wave in terms of the current−potential response suggests very weak intramolecular interactions between the Fc groups in $\mathbf{2}^+$ and $\mathbf{3}^+$. Attempts to determine the *n* value of these couples by constant potential coulometry were unsuccessful because the platinum complexes slowly decompose upon prolonged electrolysis. Previous study by Bard and Anson[28] showed that the current−potential responses of the polymer containing *n noninteracting* redox centers and the monomer containing one redox center are essentially the same except the current measured for the polymer (i_n) is higher than that of the monomer (i_1). The relationship between the current and number of redox centers (for cyclic voltammetry) is given by eq 3, where D_p and D_m are the diffusion coefficients of the polymer and the monomer.

$$i_n = n i_1 (D_p/D_m)^{1/2} \qquad (3)$$

The equation enables one to obtain the number of electrons (*n*) involved in the redox couples of **2** and **3** by comparing the magnitudes of the CV peak currents of the compounds (which can be viewed as a polymer with two noninteracting Fc groups) and a monomer such as ferrocene. However, this requires the predetermined knowledge of the diffusion coefficient of the Pt_2Au cluster (D_p), which is not available. We therefore attempted to estimate the *n* value for the reversible couples of **2** and **3** by comparing the area under the peak current in the differential pulse voltammogram of **2** and **3** with that of the $\mathbf{1}^+/\mathbf{1}$ couple normalized to the same complex concentration. The assumptions behind this estimation are (i) the $\mathbf{1}^+/\mathbf{1}$ and $\mathbf{1}^{2+}/\mathbf{1}^+$ couples are certainly one-electron oxidation of the ferrocenes in the Pt complex and they are well separated; (ii) given the similar molecular structures and mass of compounds **1**, **2**, and **3**, their diffusion coefficients should be similar to each other. It was found that the ratios of the area under the voltammogram for **2** and **3** versus that of $\mathbf{1}^+/\mathbf{1}$ are both 2.0. Thus the quasi-reversible waves displayed by **2** and **3** correspond to two-electron couples.

It is noted that when the anodic switching potential is extended to 1 V, complex **2** exhibits an irreversible oxidation at ~860 mV. Upon reverse scan, a small new couple is generated at ~165 mV (Figure 5c). Both peaks are also found in the CV of **3** but slightly shifted to 815 and 197 mV, respectively (SI). Since the waves are not found in the CV of **1**, they are possibly related to the Pt_2Au cluster. The Fc oxidation is unperturbed by the irreversible redox processes.

Scheme 3

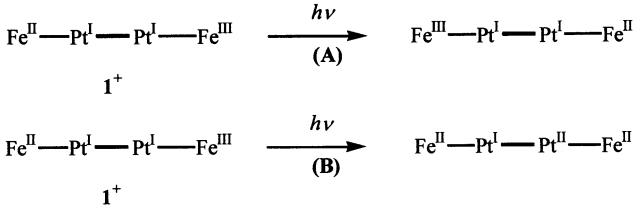

Scheme 4

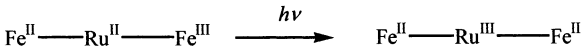

Discussion

Electronic Communication through C_2−Pt−Pt−C_2 Linkage The splitting of Fc oxidations observed in the CV of **1** indicates that the one-electron-oxidized $\mathbf{1}^+$ is more stable than the isovalent **1** and $\mathbf{1}^{2+}$, and the moderate K_c supports $\mathbf{1}^+$ being a weakly coupled class II species. Comparing the comproportionation constants of **1** and other structurally similar bis(ferrocenylacetylide) complexes (Table 3) suggests that the metal−metal interaction in $\mathbf{1}^+$ is the strongest, despite the fact that the Fe−Fe separation in **1** is the longest among them. H_{AB} of class II mixed-valence systems can be obtained from the parameters of their IVCT bands.[6a] Our study shows that $\mathbf{1}^+$ exhibits a weak absorption band at $11\,300 \pm 50$ cm^{-1} which resembles the IVCT bands of some weakly coupled class II complexes in energy and extinction coefficient.[29] Considering the electronic structure of $\mathbf{1}^+$ suggests that the absorption could originate from either one of the two charge transfer transitions depicted in Scheme 3.

Analogous complexes *trans*-$[Ru(dppm)_2(C{\equiv}CFc)_2]^+$ [9a−c] and *trans,trans*-$[Ru(PBu_3)_2(CO)(L)(C{\equiv}CFc)_2]^+$ (L = CO, pyridine, $P(OMe)_3$)[9b] can serve as benchmarks to locate the $Pt^I \rightarrow Fe^{III}$ charge transfer transition. It was shown that the $Ru^{II} \rightarrow Fe^{III}$ transitions (Scheme 4) in the complexes are intense ($\epsilon = 2900-6700$ M^{-1} cm^{-1}) and low in energy ($\nu_{max} = 4770-8030$ cm^{-1}).[9b]

The ionization potential of the low-valent third-row Pt^I is expected to be lower than that of Ru^{II}; hence the $Pt^I \rightarrow Fe^{III}$ transition, if present, should be lower in energy than the $Ru^{II} \rightarrow Fe^{III}$ transitions. Assigning the absorption to the $Pt^I \rightarrow Fe^{III}$ charge transfer transition is therefore not favored in view of its low extinction coefficient and high energy. The absorption band is ascribed to the IVCT transition from Fe^{II} to Fe^{III} (**A**). Indirect evidence for the IVCT nature of the transition comes from the absence of a similar absorption band in the spectra of one-electron-oxidized $\mathbf{2}^+$ and $\mathbf{3}^+$, which are class I mixed-valence complexes (vide infra).

(28) Flanagan, J. B.; Margel, S.; Bard, A. J.; Anson, F. C. *J. Am. Chem. Soc.* **1978**, *100*, 4748.

(29) Chen, Y. J.; Pan, D.-S.; Chiu, C.-F.; Su, J.-X.; Lin, S. J.; Kwan, K. S. *Inorg. Chem.* **2000**, *39*, 953.

Given the extinction coefficient (ϵ_{max}), absorption maxima (ν_{max}), and half-height bandwidth ($\nu_{1/2}$), the electronic coupling constant H_{AB} of $\mathbf{1}^+$ is found to be 190 ± 20 cm^{-1} using the Hush equation (eq 4),[6a] where d is the transition moment length and taken as the distance between Fe ions measured in the X-ray crystal structure (14.474(2) Å).

$$H_{AB} = \frac{2.05 \times 10^{-2}\sqrt{\epsilon_{max}(\Delta\nu_{1/2})\nu_{max}}}{d} \qquad (4)$$

The small electronic coupling constant signifies limited charge delocalization over the C≡C−Pt−Pt−C≡C backbone and confirms that $\mathbf{1}^+$ is a class II mixed-valence species. This is not unexpected given the long separation between the two iron ions, and H_{AB} is known to decrease exponentially with the intermetallic distance.[2a] In this context, it is noted that similar value of H_{AB} (290 ± 20 cm^{-1}) was found in the diferrocenylpolyene *trans*-Fc(CH=CH)$_4$Fc, which shows Fe−Fe distance = 13.87 Å, close to that in $\mathbf{1}^+$.[7e]

The stability of the mixed-valence complex is determined by several factors,[30,31] as the free energy change of the comproportionation ΔG_c ($= -RT \ln K_c = -26 \pm 1$ kJ mol^{-1}) can decompose into a statistical factor (ΔG_s), electrostatic interaction (ΔG_e), bridge-mediated electron delocalization (ΔG_{del}), an inductive effect (ΔG_{in}), and magnetic exchange (ΔG_{ex}) (eq 5).[5b,c,6e]

$$\Delta G_c = \Delta G_s + \Delta G_e + \Delta G_{del} + \Delta G_{in} + \Delta G_{ex} \qquad (5)$$

The statistical factor ΔG_s ($= -RT \ln 4$)[31] amounts to −3.4 kJ mol^{-1} at 293 K. As the comproportionation produces 2 molar equiv of $\mathbf{1}^+$, the total contribution of the other four factors per mixed-valence complex[31] should be equal to $(\Delta G_c - \Delta G_s)/2$, or -11 ± 1 kJ mol^{-1}. The electrostatic factor ΔG_e arises from the difference of intramolecular Coulomic repulsion in $\mathbf{1}^+$ and $\mathbf{1}^{2+}$. Estimation of the factor ($\Delta G_e \approx -(e^2/4\pi\epsilon r_o)$)[6e,32] is not straightforward because the dielectric constant of the molecular linkage between the terminal redox groups is unknown. However, studies on **2** and **3** show that the contribution of ΔG_e is insignificant and would not be < −2 kJ mol^{-1} (vide infra); hence the remaining factors ΔG_{del}, ΔG_{ind}, and ΔG_{ex} contribute totally about −11 to −9 kJ mol^{-1}. The factor ΔG_{del} arises from electron delocalizaion over the molecules; using eq 6,[5c] it is estimated to be -4×10^{-2} kJ mol^{-1}.

$$\Delta G_{del}(\text{cm}^{-1}) \approx -(H_{AB}{}^2/\nu_{max}) \qquad (6)$$

The above analysis shows that the two Fe centers in $\mathbf{1}^+$ interact mainly via an inductive effect (ΔG_{ind}) *and/or* magnetic exchange (ΔG_{ex}). The inductive effect, also known as the synergetic effect, is responsible for the stability of weakly coupled systems such as $[(NH_3)_5Ru^{II}(bipy)Ru^{III}(NH_3)_5]^{5+}$, whose metal ions are connected by a π-conjugated 4,4-biypridine (bipy).[31b] In essence, the inductive effect is the stabilization of the Fe^{II} ion due to the lowering of the empty π*-orbitals of the bridge by the Fe^{III} ion. In the case of **1**, however, not only π*-orbitals of the acetylene are involved in relaying the effect, as there is mixing of orbitals with π-symmetry orbitals of the Pt−Pt bond (i.e., 6p-, dπ-, and dπ*-orbitals) inserted between the two C≡C bonds. Possibly, strong π-back-bonding interactions between the low-valent Pt^I and π*-orbitals of the acetylides would enhance the inductive effect. Magnetic exchange is either ferromagnetic or antiferromagnetic coupling of two unpaired electrons in $\mathbf{1}^{2+}$. As isolation of the dication is unsuccessful, we are unable to determine the magnitude of ΔG_{ex}.

Shutdown of Electronic Communication in $\mathbf{2}^+$ and $\mathbf{3}^+$. The unresolved Fc oxidations imply very weak interaction between the iron centers in $\mathbf{2}^+$ and $\mathbf{3}^+$. Taube[33] noted that oxidation waves of weakly interacting systems with $\Delta E_{1/2} < 70$ mV would overlap and appear as a single redox couple in CV. Since the statistical factor ΔG_s (−3.4 kJ mol^{-1}) would cause a splitting of half-wave potentials ($\Delta E_{1/2}$) of 35 mV, the other factors would not be more than ∼35 mV. In other words, the total contribution of ΔG_{del}, ΔG_{ind}, ΔG_e, and ΔG_{ex} to the stability of $\mathbf{2}^+$ and $\mathbf{3}^+$ would not be < −2 kJ mol^{-1}. This result provides an estimation of the factor ΔG_e for $\mathbf{1}^+$ mentioned in the previous section. The factor ΔG_e favors the formation of the mixed-valence $\mathbf{1}^+$from $\mathbf{1}^{2+}$, as electrostatic repulsion in $\mathbf{1}^+$ ($G_e \approx 0$) is less than that in $\mathbf{1}^{2+}$ ($G_e \approx e^2/4\pi\epsilon r_o$). The through-space repulsion is a function of the distance between the point charge in $\mathbf{1}^{2+}$ (r_o) and dielectric constant ϵ between them. Given the similar Fe−Fe distances and molecular composition of **1** and the two A-frames, the electrostatic repulsion energy in $\mathbf{1}^{2+}$ and $\mathbf{2}^{2+}$ would be similar. In other words, the factor ΔG_e in $\mathbf{1}^+$ should not be < −2 kJ mol^{-1}.

In accord with the electrochemical results, no IVCT absorption band is observed in the solution of **2** and excess FcH·PF$_6$. In other words, addition of the d^{10} AuCl/Br fragment to the Pt−Pt bond switches off the electronic coupling, and $\mathbf{2}^+$ and $\mathbf{3}^+$ are class I mixed-valence complexes in which valency is trapped.

The shutdown of electronic communication in $\mathbf{2}^+$ and $\mathbf{3}^+$ is most likely due to different electronic structures of the Pt_2Au clusters. Following the results of an early theoretical study[34] on A-frame complexes, it was suggested that the interactions between the Au^I ion and the Pt−Pt bond involve mainly the orbitals in a_1-symmetry, namely, the empty 6s- and 6p$_z$-orbitals of Au^I and the dσ-orbtial of the Pt−Pt bond.[19] In line with the results, a more recent SCF-Xα-SW calculation[35] performed on the model compound $[Pt_2(\mu\text{-AuCl})(H_2PCH_2PH_2)_2Cl_2]$ showed that interactions between an Au^I ion and the Pt−Pt bond stabilize the Pt orbitals and introduce significant Au character into them, especially the dσ-orbital. As the Pt−Pt bond lies along the pathway through which the two terminal Fc groups interact, any changes in energy and parentage of the Pt orbitals are expected to affect the extent of electronic coupling. While changes in the σ-symmetry orbitals would affect the electronic communications as a whole, we believe that it is the bent geometry of A-frame **2** and **3** that

(30) Palaniappan, V.; Singru, R. M.; Agarwala, U. C. *Inorg. Chem.* **1988**, *27*, 181.
(31) (a) Sutton, J. E.; Sutton, P. M.; Taube, H. *Inorg. Chem.* **1979**, *18*, 1017. (b) Sutton, J. E.; Taube, H. *Inorg. Chem.* **1981**, *20*, 3125.
(32) (a) Ferrere, S.; Elliott, C. M. *Inorg. Chem.* **1995**, *35*, 5818. (b) Reimers, J. R.; Hush, N. S. *Inorg. Chem.* **1990**, *29*, 3686.
(33) Richardson, D. E.; Taube, H. *Inorg. Chem.* **1981**, *20*, 1278.
(34) Hoffman, D. M.; Hoffmann, R. *Inorg. Chem.* **1981**, *20*, 3543.
(35) Toronto, D. V.; Balch, A. L.; Tinti, D. S. *Inorg. Chem.* **1994**, *33*, 2507.

specifically upsets the delocalization of electron and transmission of the inductive effect. Unlike compound **1**, wherein the FcC≡C groups and the metal−metal are aligned linearly, the two FcC≡C groups in **2** and **3** deviate from the Pt−Pt bond by ∼30°. This bent configuration would reduce the overlap of the π-orbitals across the Pt−Pt bond. Disruption of π-overlap reportedly caused decrease in electronic communications in some mixed-valence complexes.[9b,36] The inductive effect, which is transmitted through the π-symmetry orbitals of the bridge, would be significantly affected by the interruption at the Pt_2Au center.

Conclusions

Our study showed that the Pt−Pt σ-bond in conjunction with C≡C bonds mediates ground state electronic interactions mostly via inductive and/or magnetic exchange. Addition of a d^{10} Au^{I} fragment to the metal−metal bond turns off the electronic communication. It is argued that the disruptions of π-conjugation and the interception by the Au orbitals switch off the electronic communication in the A-frame clusters. Charge delocalization over the C≡C−Pt−Pt−C≡C linkage is limited, as illustrated by the small H_{AB}. However it does not necessarily mean that the linkage is a poor electron-conducting pathway, as the small H_{AB} is likely due to long separation of the redox centers and indirect coupling between the redox centers and the bridge. It is envisioned that a system that allows more direct interaction between the Fe centers and the C≡C−Pt−Pt−C≡C linkage (i.e., Fe^{II}−C≡C−Pt−Pt−C≡C−Fe^{III}) would lead to a larger extent of electron delocalization. It is also interesting to know how the nature of the metal−metal bond affects the electron delocalization. For example, it would be meaningful to compare the Pt^{I}−Pt^{I} bond with other d^9−d^9 bonds such as Pd^{I}−Pd^{I} and Au^{II}−Au^{II} in their ability to mediate electron delocalization.

Acknowledgment. J.H.K.Y. thanks The National University of Singapore. K.Y.W. acknowledges the support from the Hong Kong Polytechnic University. We are grateful to Ms. Tan Geok Kheng (NUS) for her assistance with X-ray crystal structure determination.

Supporting Information Available: Tables of crystallographic data collection parameters, atomic coordinates, and a complete listing of bond lengths and bond angles for **1**·Et_2O, **2**, and **3** and CVs and DPV of compound **3**. This material is available free of charge via the Internet at http://pubs.acs.org.

OM020513+

(36) Ung, V. A.; Cargill Thompson, A. M. W.; Bardwell, D. A. Gatteschi, D.; Jeffrey, J. C.; McCleverty, J. A.; Totti, F.; Ward, M. D. *Inorg. Chem*. **1997**, *36*, 3447.